AAPS PharmSciTech, Vol. 15, No. 1, February 2014 (© 2013)
DOI: 10.1208/s12249-013-0046-y

Research Article

Physicochemical Characterization of 9-Aminocamptothecin in Aqueous Solutions

Shahidur Rahman,[1] Deval Patel,[1] and Michalakis Savva[1,2,3]

Received 12 July 2013; accepted 14 October 2013; published online 3 December 2013

Abstract. The present manuscript provides a detailed physicochemical and thermodynamic characterization of 9-aminocamptothecin (9AC) which can be used as a tool to develop novel formulation strategies for optimum pharmacological activity. The pK_a of 9AC was determined to be 2.43 at 37°C, while the basicity of quinoline nitrogen of 9AC was found to decrease with increasing temperature due to a positive enthalpy of deprotonation of 10.36 kJ mol^{-1}. The equilibrium solubility as well as the intrinsic solubility of the drug was found to increase with increasing temperature and decreasing pH. The enthalpies of solution of unionized and ionized forms of 9AC obtained from isothermal and iso-pH equilibrium solubility measurements were found to be 36.01 and 24.72 kJ mol^{-1}, respectively. Equilibrium hydrolysis studies revealed the hydrolytic susceptibility of 9AC with only 14% of active lactone species remaining at physiological pH 7.4. The intrinsic partition coefficient log *P* of the free base, 9AC–lactone, was estimated to be 1.28 (a characteristic of molecules suitable for oral absorption). The estimated pK_a and log *P* values of 9AC, combined with its increased solubility at lower pH, are features that can be utilized to develop novel drug delivery systems to optimize the antitumor activity of 9AC.

KEY WORDS: 9-aminocamptothecin; hydrolysis; partition coefficient; physicochemical characterization; solubility.

INTRODUCTION

In spite of being selected by the US National Cancer Institute as a high-priority antitumor compound for further clinical development, 9-aminocamptothecin (9AC) has not reached its therapeutic potential as yet, partly because of its poor aqueous solubility and hydrolytic instability at physiological pH (Scheme 1). 20(*S*)-Camptothecin (CPT), along with its various analogs, are a highly promising class of antitumor agents that inhibit the activity of topoisomerase-I by binding and stabilizing the transient DNA–topoisomerase I complex formed during the S-phase of cell replication. This ternary complex is generally referred to as the topoisomerase I cleavage complex, which involves a series of reactions ultimately leading to cell death (1–6). The closed α-hydroxy-δ-lactone ring of CPT and analogs is an important structural requirement for both passive diffusion of the drug into the cancer cells as well as for successful drug interaction with the pharmacological target, topoisomerase I (7). The drug delivery to the target site under physiological conditions is the most challenging task for CPT due to its poor water solubility and hydrolytic conversion from the active lactone to inactive carboxylate form which is up to tenfold less potent (8).

9AC is a semisynthetic analog of CPT obtained by the catalytic hydrogenation of 9-nitrocamptothecin (9NC) at C9 position (9). Various types of drug delivery systems tested in phases I and II clinical studies were developed aiming to improve the pharmacokinetics of 9AC and unleash its therapeutic potential (10–14). Like other CPT analogs, 9AC also suffers from drawbacks of low solubility and hydrolytic instability at physiological pH but, to our knowledge, no comprehensive thermodynamic studies have ever been published in the literature. There is a further need to study the behavior of 9AC in aqueous media if we are to discover novel formulation strategies for optimum *in vivo* delivery of 9AC.

In this regard, the present work is focused on a detailed investigation of the physicochemical properties of 9AC in aqueous solution. Various properties such as pK_a, partition coefficients, and effect of pH and temperature on the solubility of 9AC were determined in physiological and acidic media using a chromatographic assay for the simultaneous quantification of lactone and carboxylate species of 9AC.

MATERIALS AND METHODS

Materials

The 9AC, 4-ethyl-4-hydroxy-9-amino-1H-pyrano[3′,4′:6,7] indolizino [1,2-*b*]quinoline-3,14(4H,12H)-dione, CAS number (91421-43-1), $C_{20}H_{17}N_3O_4$, 363.37 g mol^{-1}, and mass fraction purity (≥0.99) was obtained as a gift from the US National Cancer Institute. All experiments were performed using analytical grade reagents.

[1] Division of Pharmaceutical Sciences, Arnold & Marie Schwartz College of Pharmacy & Health Sciences, Long Island University, 75 Dekalb Avenue, Brooklyn, New York 11201, USA.
[2] *Present Address:* 51 N. Pattihi, 3070, Limassol, Cyprus.
[3] To whom correspondence should be addressed. (e-mail: micsavva@gmail.com)

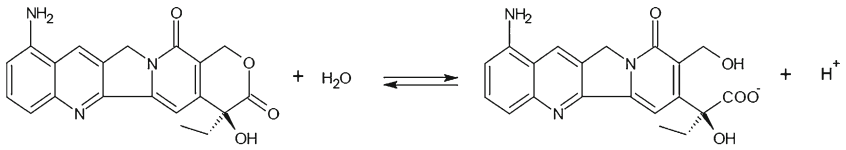

9AC-lactone 9AC-carboxylate

Scheme 1. Reversible hydrolysis reaction of 9AC–lactone to 9AC–carboxylate

Deionized water was obtained from Barnstead NANO pure water system (Barnstead, Dubuque, IA, USA). Sodium chloride was purchased from Fisher Scientific (Fair Lawn, NJ, USA). Dimethyl sulfoxide (DMSO, high-performance liquid chromatography (HPLC) grade, 99%), 1-octanol (HPLC grade, 99%), triethylamine (TEA, 99%), hydrochloric acid (1 M), and sodium hydroxide (1 M) was purchased from Sigma-Aldrich (St. Louis, MO, USA).

Methods

HPLC Instrumentation

The HPLC used for drug content analysis consisted of a Waters HPLC system (Milford, MA, USA) equipped with a 717 plus autosampler, a Spectra-Physics Spectra SYSTEM UV 1000 detector, an interface module, and a single 515 pump. Chromatographic analysis of 9AC–lactone and 9AC–carboxylate species was conducted on a Waters Symmetry® C18 analytical column (3.9×150 mm; pore size, 5 μm) using a mobile phase consisting of 80:20 *v/v* mixture of aqueous phase to acetonitrile. The aqueous phase consisted of TEA at volume fractions of 1.5%, with the pH adjusted at 5.5 using acetic acid. UV detection was carried out with the excitation wavelength set at 366 nm, while the flow rate was set at 1 mL min^{-1}. The chromatographic run time was 9 min with retention times of 2.9 and 7.3 min for 9AC–carboxylate and 9AC–lactone, respectively. Calibration curves of 9AC–lactone and 9AC–carboxylate were constructed with standard solutions in 0.001 M HCl and 0.001 M NaOH, respectively.

Equilibrium Hydrolysis Studies

Various buffer solutions of pH ranging from 2 to 10 were prepared by mixing different proportions of 0.2 M phosphate (Na_2HPO_4) and 0.1 M citric acid solutions. To these, appropriate volumes from stock solutions of the drug in DMSO (1 mg mL^{-1}) were added at a constant final concentration below the drug solubility (220 ng mL^{-1}). Samples in triplicate were vigorously shaken using an orbital shaker at room temperature for 120 h (equilibrium was reached within 72 h); after which, 9AC–lactone and 9AC–carboxylate were simultaneously quantified using an HPLC assay. Calibration curves of 9AC–lactone and 9AC–carboxylate were constructed within the range of 50.70–1,014 ng mL^{-1} of drug in standard solutions of 0.001 M HCl and 0.001 M NaOH, respectively. Percent fractional concentrations of each species were calculated upon integrating the area under each peak in the chromatogram, converting the area into species concentration using the slope of the linear fit of the calibration curve and finally dividing the given concentration by the initial concentration C_o, using, % fractional concentration $= \frac{C}{C_o} \cdot 100$.

The equilibrium hydrolysis data were fitted by Eq. (1) using the Microsoft Excel® Solver through minimization of the sum of the squared residuals with four adjustable parameters at 5% tolerance level.

$$A = A_{\min} + \frac{A_{\max} - A_{\min}}{1 + 10^{c \cdot (\mathrm{pH} - D)}} \quad (1)$$

Where A is the calculated equilibrium percentage 9AC–lactone or 9AC-carboxylate, $A_{\max}$ and $A_{\min}$ are the maximum and minimum percent concentrations, and D is the adjustable parameter referring to the pH at which equilibrium concentrations of 9AC–lactone and 9AC–carboxylate are equal. The parameter c is included in Eq. (1) to account for non-ideal experimental conditions and better optimize the curve fitting of the data by iteration. Ideally, c is equal to +1 or −1, depending on whether the drug is a weak acid or a base.

pK_a Studies

A Cary eclipse UV-spectrophotometer (Varian Inc., Walnut Creek, CA, USA) was used to record the spectral scans of 9AC–lactone in different pH solutions at 37°C. Various pH solutions in the range of 0.2–3.6, all containing 3.5 μg mL^{-1} of 9AC–lactone that was transferred from a 1 mg mL^{-1} stock solution in DMSO, were made by adding appropriate volumes of 1 M HCl in HPLC-grade water. Samples in triplicate were stirred for 30 min, absorbance values of the spectral scans at $\lambda_{\max}$ of the ionized form were recorded and simultaneously fitted by the Henderson–Hasselbalch Eq. (1) using Microsoft Excel® solver function, as described in the previous section. In this case, the adjustable parameter D represents the pK_a of 9AC–lactone.

Partition Coefficient Studies

The partition coefficient of 9AC was determined by the shake flask method. Briefly, 22 μL of 9AC–lactone was transferred from 0.1 mg mL^{-1} stock solution in DMSO to 10 mL of 1-octanol (organic phase) and aqueous phase (5 mL each phase) in 15-mL-capacity polypropylene conical tubes and vigorously shaken for 24 h on an orbital shaker at room temperature. To accurately determine the intrinsic partition coefficient of the unionized 9AC–lactone form, the pH of the aqueous phases during the initial studies was adjusted in the range of 1.5–2.0 units above and below the pK_a value of the quinoline nitrogen of 9AC–lactone with 1 M HCl solution. Samples were allowed to equilibrate for an

additional 24 h at room temperature; after which, the aqueous phase was analyzed for drug concentration using an HPLC assay. The concentration of 9AC in aqueous phase was determined from the slopes of calibration curves constructed at each pH, while the concentration of 9AC in octanol was determined from the difference of the total amount of drug added and the amount present in the aqueous phase.

The apparent partition coefficient (P_{app}) of 9AC was calculated from the concentrations of 9AC in the octanol $[C_u]_o$ and aqueous phase $[C_{total}]_w$, according to the following equation,

$$P_{app} = \frac{[C_u]_o}{[C_{total}]_w} = \frac{[9AC{-}lactone]_o}{[9AC{-}lactone]_w + [9ACH{-}lactone]_w^+} \quad (2)$$

The intrinsic partition coefficient P of the unionized form of 9AC–lactone and pK_a were obtained from the intercept and slope, respectively, using the linear fit of the experimental data by Eq. (3),

$$P_{app} = \frac{P}{1 + 10^{(pK_a - pH)}} \quad (3)$$

Experimental data were plotted by using the linear fit of Eq. (4) and the intrinsic partition coefficient of the unionized and ionized form of the drug, P and P', were determined from the slope and the intercept.

$$P_{app} \cdot \left(1 + \frac{K_a}{[H^+]}\right) = P' + P \cdot \left(\frac{K_a}{[H^+]}\right) \quad (4)$$

Where, $P_{app} = \frac{[C_u]_o + [C_i]_o}{[C_u]_w + [C_i]_w}$, $P = \frac{[9AC\text{–}lactone]_o}{[9AC\text{–}lactone]_w}$ and $P' = \frac{[9ACH\text{–}lactone]_o^+}{[9ACH\text{–}lactone]_w^+}$. The concentrations $[C_i]_w$ and $[C_i]_o$ are those of the ionized drug species in the aqueous and organic phase (Scheme 2), respectively, while $[C_u]$ denotes the concentration of unionized 9AC–lactone-free base.

Solubility Studies

The procedure was similar to that described elsewhere (8). Briefly, excess 9AC powder was suspended in 25 mL of dissolution media in temperature regulated Kontes jacketed beakers (VWR brand, model 1162, PolyScience, IL, USA). The ionic strength of the media was maintained constant at 0.3 M using NaCl, while the pH of the dissolution media were adjusted to pH 1.2, 2.0, 2.4, 3.0, and 4.4 using 1 M HCl. Solvent evaporation during the experiment (72 h) was prevented by covering the beakers with paraffin film. At predetermined time intervals, aliquots (5 mL) were withdrawn from the beaker, filtered using a Life Science Acrodisc® Syringe Filter (25 mm diameter and 0.2 μm pore size) and analyzed by HPLC. The solubility studies were also performed at multiple temperatures in order to evaluate the effect of heat on 9AC dissolution rates and saturated concentration.

Measured 9AC concentrations (C_T) were plotted against the calculated hydronium concentration, $[H^+]$, and data were fitted by Eq. (5) using linear regression analysis. The intrinsic solubility of the 9AC–lactone-free base, [9AC–lactone], and the dissociation constant K_a were determined from the intercept and slope of the Eq. (5),

$$C_T = [9AC\text{–}lactone] \cdot \left(1 + \frac{[H^+]}{K_a}\right) \quad (5)$$

C_T is the total solubility of 9AC equaled to the sum of [9AC–lactone]+[9ACH–lactone]$^+$, where [9ACH–lactone]$^+$ denotes the protonated form of 9AC.

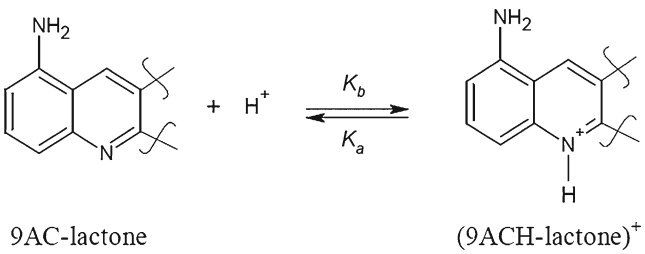

Scheme 2. Ionization reaction of quinoline nitrogen of 9AC

RESULTS AND DISCUSSION

Equilibrium Hydrolysis Studies

Nonlinear curve fitting of the 9AC–lactone and 9AC–carboxylate equilibrium concentrations by Eq. (1), indicates that 9AC–lactone is stable below pH 4.5 (Fig. 1). There is a reversible and exponential decrease in the equilibrium lactone concentration from pH 5–7, with only 14.4% of 9AC–lactone remaining at the physiological pH 7.4. This is comparable to the stability of other CPT analogs, *e.g.*, CPT (22.91%) (15), 10-HC (18%) (8), SN38 (15.1%) (16), and 9NC (10%) (unpublished results). Furthermore, above pH 8.5, 9AC is exclusively present in its inactive, polar carboxylate form.

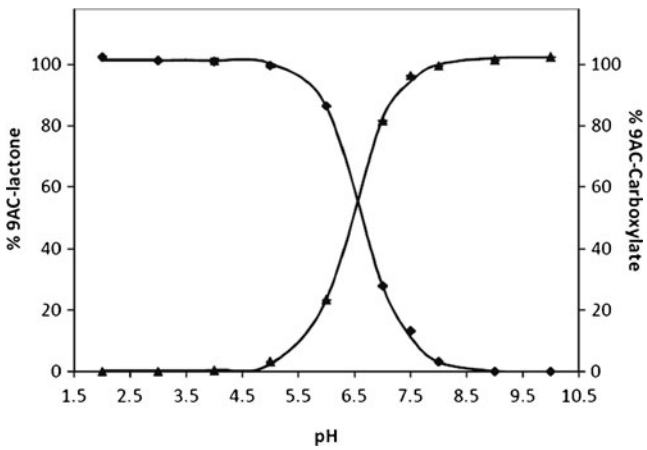

Fig. 1. Equilibrium concentrations of 9AC–lactone (*black diamond*) and 9AC-carboxylate (*black triangle*) plotted as a function of pH at room temperature. The percentage of each chemical species was calculated by multiplying the corresponding fractional concentrations by 100. *Solid lines* represent best fits of the 9AC–lactone and 9AC–carboxylate by Eq. (1). *Error bars* are the standard deviations from three independent experiments

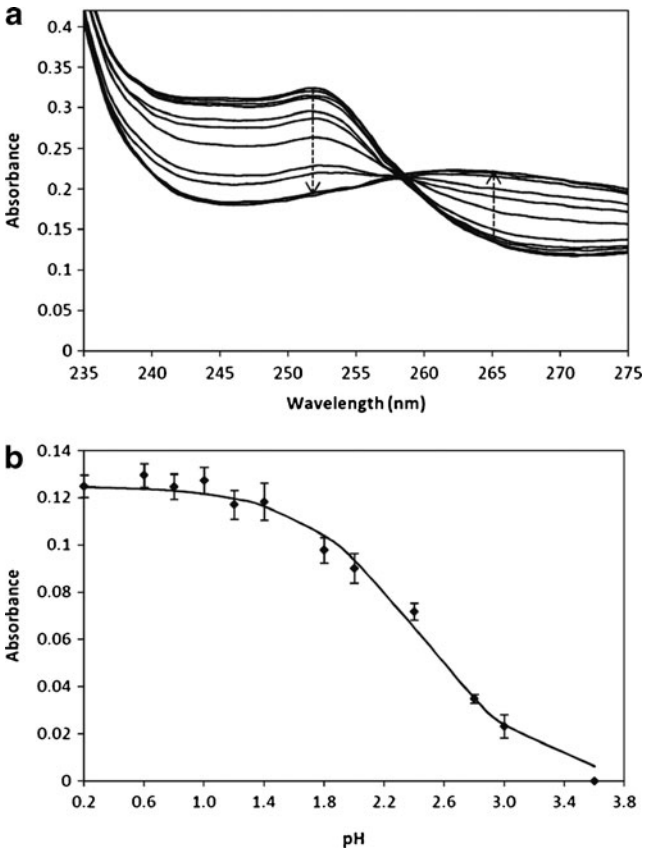

Fig. 2. **a** pH-dependent changes of the UV absorption of 9AC (3.5 μg mL^{-1}) at 37°C. The direction of the *arrows* indicates increasing pH from 0.2 to 3.6. **b** Absorbance of 9AC–lactone at 252 nm plotted as a function of pH. Results are the average of three independent experiments with the error bars representing standard uncertainties. Best fit of the data by Eq. (1) is shown with *solid line*

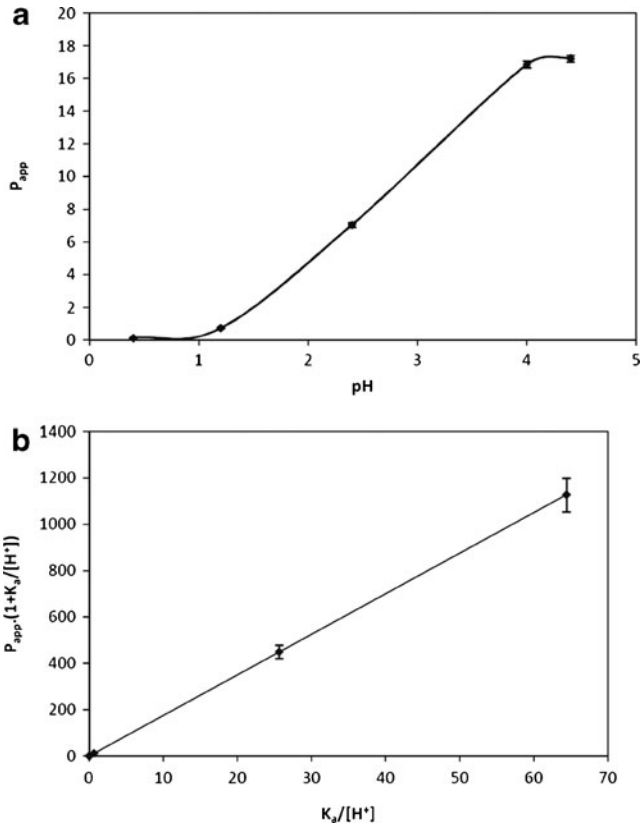

Fig. 3. **a** Plot of apparent partition coefficients (*black diamond*) as a function of pH at 298.15 K. Simulated results are represented by *solid line*. *Error bars* are the standard deviations calculated from three independent experiments. **b** Extension of the theory to octanol/water partitioning of the ionized solute $(9ACH\text{-lactone})^+$. Experimental data (*black diamond*) at 298.15 K were fitted by Eq. (4) (*solid line*)

Based on the equilibrium hydrolysis results of other analogs, 9AC appears to be slightly less stable at physiological pH.

pK_a Studies

The absorption spectra of 9AC have a λ_{max} at 252 nm. The UV spectra of 9AC revealed the presence of one isosbestic point within the pH range of 0.2–3.6, suggesting the existence of only two species, *i.e.*, protonated and unprotonated quinoline nitrogen of the 9AC–lactone (Fig. 2a, Scheme 2). Plotting the 9AC representative absorbance values at 37°C as a function of pH and fitting these values by the modified Henderson–Hasselbalch equation (Eq. 1) yielded an average pK_a value of the quinoline nitrogen of 9AC of 2.43 (Fig. 2b).

Partition Coefficient Studies

The results derived from the partition experiments (Fig. 3a) provided an initial estimate of the intrinsic partition coefficient of the unionized 9AC–lactone. All measurements were performed at pH where the 9AC–lactone form is stable, and at pH close to the vicinity of pK_a. The apparent partition coefficient P_{app} was first calculated by Eq. (2). Linear regression analysis of the calculated inverse values of the apparent partition coefficient plotted against the calculated hydrogen concentration by Eq. (3), yielded average values of intrinsic partition coefficient P of the unionized form of 9AC–lactone and pK_a, equal to 18.49 and 2.59, respectively. To account for possible partitioning of the protonated form of 9AC into the octanol phase, the calculated apparent partition coefficient, P_{app}, was plotted as shown in Fig. 3b. The initial estimate of P value and pK_a obtained from Eq. (3) was applied to Eq. (4), and the experimental data were fitted by Eq. (4) with three adjustable parameters at 5% tolerance. The intrinsic partition coefficient P' of the ionized 9AC-lactone, $[9ACH\text{-lactone}]^+$, was calculated to be 0.26. Comparison of the P values of 9AC with the parent compound CPT and other camptothecin derivatives is quite insightful. Firstly, the much higher P values of SN38 and CPT (2333 and 52 *versus* 18 for 9AC) (15,16), suggest that the amino group substitution greatly increases the polar surface area of the 9AC resulting in decreased lipophilicity and cell membrane permeability. On the other hand, the higher lipophilicity of 9AC compared to 10HC (P value of 6.2) (8) could prove advantageous for oral delivery yielding a better absorption profile in the acidic environment of the stomach, since the low pK_a value of 9AC guaranties at least 50% of the lactone form of 9AC to exist as a free base. Interestingly, 9NC does not seem to suffer from this disadvantage though it has similar octanol/water partition value as that of 9AC, but its pK_a value is −0.3 (unpublished results), thus 100% of 9NC exists in the acidic environment of the stomach as a free base.

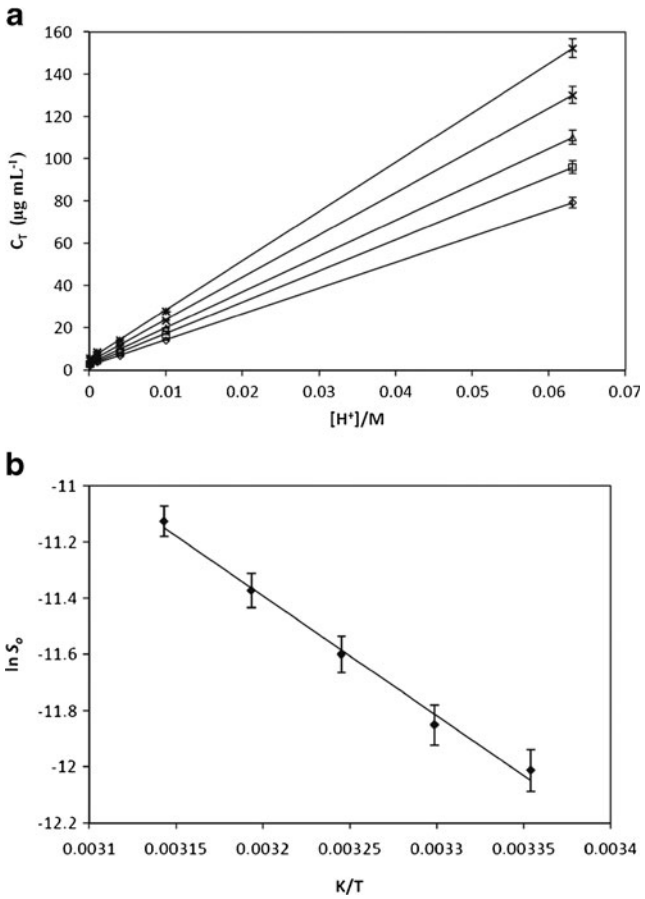

Fig. 4. **a** Isotherms of total solubility of 9AC–lactone, C_T *versus* calculated hydrogen ion concentration, [H$^+$] at 298.15 K (*white diamond*), 303.15 K (*white square*), 308.15 K (*white triangle*), 313.15 K (*multiplication symbol*), and 318.15 K (*asterisk*). **b** Plot of 9AC–lactone intrinsic solubility, lnS_o as a function of inverse temperature. Data are the average of three independent experiments with *error bars* representing standard deviations

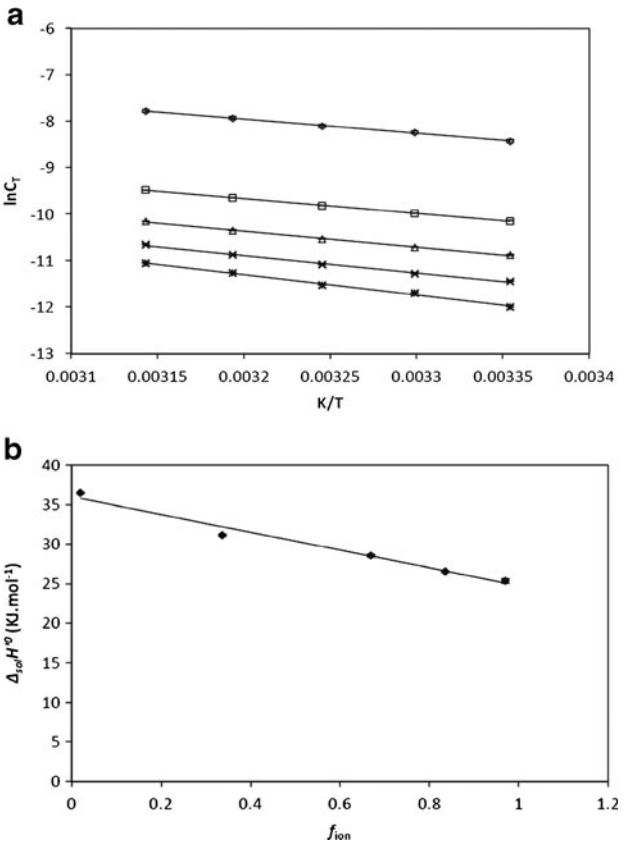

Fig. 5. **a** Iso-pH plots of 9AC–lactone saturated concentration, lnC_T as a function of inverse temperature measured in solutions of pH 1.2 (*white diamond*), 2.0 (*white square*), 2.4 (*white triangle*), 3.0 (*multiplication symbol*), and pH 4.4 (*asterisk*). **b** Enthalpy of dissolution plotted as a function of fraction of 9AC-lactone ionized (f_{ion}) that was calculated from the pK_a values at various temperatures using the Henderson–Hasselbalch Eq. (1). Results were fitted by Eq. (7). Error bars are the standard deviations calculated from the average values of three independent experiments

Solubility Studies

Saturated concentrations C_T of 9AC were measured at various temperatures in acidic solutions and plotted as a function of pH (Fig. 4a). Results were fitted using Eq. (5) and the intrinsic solubility of 9AC-lactone and pK_a were calculated from the intercepts and slopes of the various isotherms, respectively. In close agreement with the pK_a values obtained from UV-spectroscopy and octanol–water partition studies, the apparent pK_a was determined to be 2.74±0.05 at 298.15 K. As shown in Table I, the apparent pK_a of 9AC–lactone decreased marginally with increasing temperatures; nonetheless, the trend was clear, more subtle but similar to that of 10HC and SN38 (8,16). Linear fitting of the plot lnK_a against 1/T yielded an enthalpy of protonation or ionization $\Delta_{ion}H'^{\circ}$ equal to −10.36 kJ mol^{-1} with a correlation coefficient of 0.89. The equilibrium solubility of 9AC–lactone at pH 1.2 increased from 79.26 μg mL^{-1} at 298.15 K to 152.2 μg mL^{-1} at 318.15 K. Contrary to that, at 298.15 K and pH 4.4, the solubility of the 9AC–lactone increased approximately 35 times from 2.24 μg mL^{-1} as a free base to 79.26 μg mL^{-1} at pH 1.2, which is predominantly present as an

Table I. Intrinsic Solubility of Unionized Species of 9AC–lactone and Ionization Constants as a Function of Temperature

T/K	pK_a	Intrinsic solubility, S_o/(μg mL^{-1})
298.15	2.74±0.05	2.21±0.16
303.15	2.71±0.09	2.60±0.18
308.15	2.70±0.04	3.34±0.2
313.15	2.68±0.04	4.19±0.25
318.15	2.69±0.09	5.35±0.28

Table II. Heat of Solution, $\Delta_{sol}H'^{o}$ of (Ionized+Unionized) Species as a Function of pH

pH	$\Delta_{sol}H'^{o}$/kJ mol^{-1}
1.2	25.39±0.26
2.0	26.54±0.05
2.4	28.56±0.15
3.0	31.15±0.13
4.4	36.48±0.06

ionized salt. Clearly, salt formation is a much more efficient way of solubilizing the 9AC than increasing the temperature of the aqueous solution. Due to the endothermic nature of the dissolution process, the intrinsic solubility of the unionized lactone increased linearly with temperature to about 2.4 times its magnitude from 298.15 to 318.15 K (Table I). Intrinsic solubilities of the unionized species of 9AC were plotted as a function of inverse absolute temperature, and the experimental data were fitted by the integrated form of the Gibbs–Helmholtz equation Eq. (6) (Fig. 4b). The apparent average standard enthalpy of the solution $\Delta_{sol}H'^{o}_{un}$ of the unionized 9AC–lactone calculated from the slope of the linear fit was found to be 35.4 kJ mol^{-1}. C(T) is a constant as a function of the temperature (8),

$$\ln S_o = -\frac{\Delta_{sol}H'^{o}_{un}}{R}\cdot\frac{1}{T} + C(T) \quad (6)$$

The temperature dependence of equilibrium solubility of 9AC at different pH is shown in Fig. 5a. The apparent standard enthalpy of solution $\Delta_{sol}H'^{\circ}$ containing both unionized and ionized 9AC–lactone molecules was calculated from the slopes of the linear fits of iso-pH saturated concentrations of 9AC–lactone at various temperatures. As shown in Table II, the apparent standard enthalpy of solution increases with increasing pH, suggesting that the dissolution of unionized species is energetically more demanding than the ionized form of 9AC–lactone.

A plot of the $\Delta_{sol}H'^{o}$ against the fraction ionized f_{ion} and a least-squares fitting of the data according to Eq. (7), is shown in Fig. 5b. The intercept of the linear fit yielded an apparent average standard enthalpy of the solution $\Delta_{sol}H'^{o}_{un}$ of the unionized 9AC–lactone equal to 36.01 kJ mol^{-1}, while the slope of the fit yielded an average value of the apparent standard heat of solution of the ionized lactone species, $\Delta_{sol}H'^{o}_{ion}$, equal to 24.72 kJ mol^{-1}.

$$\Delta_{sol}H'^{o} = \left(\Delta_{sol}H'^{o}_{ion} - \Delta_{sol}H'^{o}_{un}\right)\cdot f_{ion} + \Delta_{sol}H'^{o}_{un} \quad (7)$$

Thus, although the solubility of both species is an endothermic process, dissolution of protonated species is evidently less dependent on temperature due to the negative heat of ionization $\Delta_{ion}H'^{o}$ (−10.36 kJ mol^{-1}). Due to the much bigger positive enthalpy of dissolution of the free base, the pH-dependent total solubility of 9AC increases with increasing temperature.

Further comparison of 9AC with other analogs of CPT revealed that at 298.15 K and pH 2, the equilibrium solubility of 9AC (14.16 mg L^{-1}) was 17 times higher compared to that of 10HC (0.83 mg L^{-1}) (8) and 70.8 times higher compared to that of SN38 (0.2 mg L^{-1}) (16). This higher equilibrium solubility of 9AC can be attributed to its higher pK_a and higher intrinsic solubility as compared to that of 10HC and SN38.

In short, a number of properties indispensable to formulation scientists were determined. We have shown that 9AC–lactone is stable below pH 4.5 and hence, the delivery of the pharmacologically active form, in the absence of any carriers, requires the use of acidic aqueous media. Furthermore, the fact that at physiological pH, only 14% of 9AC was present in its active lactone form, suggests that efficient delivery of 9AC in media of neutral pH can only be achieved with carriers that bind and encapsulate 9AC, thus preventing its hydrolysis. However, loading high amounts of 9AC–lactone into delivery systems to reach therapeutic doses will also require the use of highly acidic media. This idea is further reinforced by the solubility studies which indicated that 9AC solubility is more enhanced in acidic pH than at elevated temperatures. There was a 35-fold increase in solubility of 9AC when the pH was decreased from 4.4 to 1.2 at 298.15 K compared to only 1.9-fold increase in solubility when the temperature was increased from 298.15 to 318.15 K at pH 1.2. Considering that the log *P* value of 9AC is 1.28 and its pK_a is 2.43, a per oral administration of a 9AC acidic aqueous solution, free or encapsulated into other carriers, may not be a bad idea. 9AC will stay ionized and soluble in the acidic gastric environment until it transits to the intestine.

CONCLUSION

9AC was found to be stable in its lactone form below pH 4.5. The enthalpies of solution of the ionized and unionized species of 9AC indicated that dissolution of 9AC is an endothermic process even though the heat of protonation of the quinoline nitrogen of 9AC is negative. The pK_a of 9AC–lactone was determined to be 2.43 at physiological temperature, which is significantly higher than the values of CPT and 10HC (1.2 and 1.42, respectively) (8,15,17). Detailed analysis of solubility measurements combined with partition coefficient studies revealed that not only 9AC is more polar than the parent CPT but it also possesses considerably higher equilibrium solubility in aqueous media compared to that of 10HC and SN38. The higher lipophilicity coupled with the higher pK_a value of 9AC, compared to that of 10HC, can be exploited to develop an optimum oral drug delivery system.

ACKNOWLEDGMENTS

We are grateful to the US National Cancer Institute for providing 9-aminocamptothecin used in this entire work.

REFERENCES

1. Venditto VJ, Simanek EE. Cancer therapies utilizing the camptothecins: a review of the in vivo literature. Mol Pharm. 2010;7(2):307–49.
2. Moukharskaya J, Verschraegen C. Topoisomerase 1 inhibitors and cancer therapy. Hematol Oncol Clin North Am. 2012;26(3):507–25.
3. Pommier Y, Leo E, Zhang H, Marchand C. DNA topoisomerases and their poisoning by anticancer and antibacterial drugs. Chem Biol. 2010;17(5):421–33.
4. Bailly C. Topoisomerase I, poisons and suppressors as anticancer drugs. Curr Med Chem. 2000;7(1):39–58.
5. Nakagawa H, Saito H, Ikegami Y, Aida-Hyugaji S, Sawada S, Ishikawa T. Molecular modeling of new camptothecin analogues to circumvent ABCG2-mediated drug resistance in cancer. Cancer Lett. 2006;234(1):81–9.
6. Pommier Y. Topoisomerase I, inhibitors: camptothecins and beyond. Nat Rev Cancer. 2006;6(10):789–802.
7. Burke TG, Mi Z. The structural basis of camptothecin interactions with human serum albumin: impact of drug stability. J Med Chem. 1994;37(1):40–6.

8. Kunadharaju S, Savva M. Thermodynamic studies of 10-hydroxy-camptothecin in aqueous solutions. J Chem Eng Data. 2010;55(1):103–12.
9. Wani MC, Nicholas AW, Wall ME. Plant antitumor agents. 23. Synthesis and antileukemic activity of camptothecin analogues. J Med Chem. 1986;29(11):2358–63.
10. Bartlett NL, Johnson JL, Wagner-Johnston N, Ratain MJ, Peterson BA. Phase II study of 9-aminocamptothecin in previously treated lymphomas: results of Cancer and Leukemia Group B 9551. Cancer Chemother Pharmacol. 2009;63(5):793–8.
11. Gao SQ, Lu ZR, Petri B, Kopeckova P, Kopecek J. Colon-specific 9-aminocamptothecin-HPMA copolymer conjugates containing a 1,6-elimination spacer. J Control Release. 2006;110(2):323–31.
12. Miller DS, Blessing JA, Waggoner S, Schilder J, Sorosky J, Bloss J, *et al*. Phase II evaluation of 9-aminocamptothecin (9-AC, NSC #603071) in platinum-resistant ovarian and primary peritoneal carcinoma: a Gynecologic Oncology Group Study. Gynecol Oncol. 2005;96(1):67–71.
13. Xiong HQ, Tran HT, Madden TL, Newman RA, Abbruzzese JL. Phase I and pharmacological study of oral 9-aminocamtothecin colloidal dispersion (NSC 603071) in patients with advanced solid tumors. Clin Cancer Res. 2003;9(6):2066–71.
14. Leguizamo J, Quinn M, Takimoto CH, *et al.* A phase I study of 9-aminocamptothecin as a colloidal dispersion formulation given as a fortnightly 72-h infusion. Cancer Chemother Pharmacol. 2003;52(4):333–8.
15. Selvi B, Patel S, Savva M. Physicochemical characterization and membrane binding properties of camptothecin. J Pharm Sci. 2008;97(10):4379–90.
16. Thakur R, Sivakumar B, Savva M. Thermodynamic studies and loading of 7-ethyl-10-hydroxycamptothecin into mesoporous silica particles MCM-41 in strongly acidic solutions. J Phys Chem B. 2010;114(17):5903–11.
17. Fassberg J, Stella VJ. A kinetic and mechanistic study of the hydrolysis of camptothecin and some analogues. J Pharm Sci. 1992;81(7):676–84.